

Striped superconductors in the extended Hubbard model.

Ivar Martin, Gerardo Ortiz, A. V. Balatsky, and A. R. Bishop
Theoretical Division, Los Alamos National Laboratory, Los Alamos, NM 87545
(December 2, 2024)

We present a minimal model of a doped Mott insulator that simultaneously supports antiferromagnetic stripes and d -wave superconductivity. We explore the implications for the global phase diagram of the superconducting cuprates. At the unrestricted mean-field level, the various phases of the cuprates, including weak and strong pseudogap phases, and two different types of superconductivity in the underdoped and the overdoped regimes, find a natural interpretation. We argue that on the underdoped side, the superconductor is intrinsically inhomogeneous – striped coexistence of superconductivity and magnetism – and the global phase coherence is achieved through the Josephson-like coupling of the superconducting stripes. On the overdoped side, the state is overall homogeneous and the superconductivity is of the classical BCS type.

Experimental evidence increasingly suggests that microscopic inhomogeneous “stripe” states are ubiquitous in the doped cuprates, as well as in other complex electronic materials [1]. Nanoscale stripe morphologies have been observed in YBCO and LSCO in neutron scattering and angle resolved photoemission experiments. In the superconducting phase, the stripes appear to coexist with superconductivity in a range of dopings without destroying the global phase coherence. The main issue that we address in this Letter is the nature of the superconducting state in the presence of stripes.

Inhomogeneous quantum states in non-superconducting lattice models are no less common than they are in the experiments. Many lattice models possessing antiferromagnetic (AF) ground states at half-filling, when doped away from that filling develop stripes at the unrestricted mean-field (MF) level [2–4]. Exact solutions may lead to fluctuations that introduce dynamics into the idealized MF solutions, but are expected to preserve at least some qualitative features of the MF. The lower the spatial dimension the more important the quantum fluctuations are and, sometimes, MF solutions do not reproduce the exact large distance physics of the problem. However, often they pick up the low lying manifold of excited states which becomes relevant at low enough temperatures. Also, 3-dimensional coupling in real materials helps to reduce the effect of fluctuations.

We consider here a minimal model with stripes to illustrate our conclusions. We employ the 2-dimensional one-band Hubbard Hamiltonian with hopping t and on-site repulsion U [2]. Superconductivity is introduced by including the nearest neighbor attraction V , which produces pairing predominantly in the d -wave channel close to half-filling [5]. The effective minimal Hamiltonian is thus

$$H = -t \sum_{\langle ij \rangle \sigma} c_{i\sigma}^\dagger c_{j\sigma} + U \sum_i n_{i\uparrow} n_{i\downarrow} - V \sum_{\langle ij \rangle} n_i n_j, \quad (1)$$

where the operator $c_{i\sigma}^\dagger$ ($c_{j\sigma}$) creates (annihilates) an electron with spin σ on the lattice site i , and $n_i =$

$c_{i\uparrow}^\dagger c_{i\uparrow} + c_{i\downarrow}^\dagger c_{i\downarrow}$ represents the electron density on site i . For our computations, we use the unrestricted mean-field approximation to this Hamiltonian,

$$H_{MF} = -t \sum_{\langle ij \rangle \sigma} c_{i\sigma}^\dagger c_{j\sigma} + U \sum_i n_{i\uparrow} \langle n_{i\downarrow} \rangle + \langle n_{i\uparrow} \rangle n_{i\downarrow} - \sum_{\langle ij \rangle} c_{i\downarrow} c_{j\uparrow} \Delta_{ij}^* + \text{H.c.}, \quad (2)$$

where $\Delta_{ij} = V \langle c_{i\downarrow} c_{j\uparrow} \rangle$ is the MF superconducting order parameter. The direct Hartree terms in V are neglected since the magnitude of the effective nearest neighbor attraction is expected to be much smaller than the on-site repulsion U . Hence, it should not affect the diagonal part of the Hamiltonian, which is responsible for the charge and spin order. Therefore, the effect of V in our model is limited to the generation of any anomalous correlations. We do not address the very important issue of the microscopic origin of the attraction V . Our goal is only to construct a minimal model that may help to qualitatively understand the rich phase diagram of the cuprates. Unless stated otherwise, standard parameter values used are $U = 4t$ and $V = -0.9t$. This choice of parameters allows us to demonstrate our conclusions regarding the inhomogeneous superconducting phase more clearly.

To self-consistently solve the MF equations we use an iterative scheme. This consists of two stages which are repeated until convergence is achieved: (1) Diagonalization of the MF Hamiltonian. (2) Update of the MF parameters. An important feature of our approach is that all physical quantities are allowed to vary from one lattice site to another, e.g., $\langle n_{i\uparrow} \rangle \neq \langle n_{i\downarrow} \rangle$ and $\langle n_{i\sigma} \rangle \neq \langle n_{i+\alpha\sigma} \rangle$. Generically, we are looking for inhomogeneous solutions whose typical correlation lengths ξ involve several lattice spacings. Therefore, it is important that the simulated supercell size $N_x \times N_y$ (with periodic boundary conditions) is such that $N_{x,y} > \xi_{x,y}$. The Hamiltonian in Eq. (2) can be rewritten in the matrix form, $H_{MF} = \mathbf{c}^\dagger \hat{H} \mathbf{c}$, with $\mathbf{c} = (c_{1\uparrow}, c_{1\downarrow}, c_{2\uparrow}, c_{2\downarrow}, \dots)^T$, where

\hat{H} is a $(2N_xN_y) \times (2N_xN_y)$ hermitian matrix. By applying a unitary transformation α ($\alpha^{-1} = \alpha^*$) the Hamiltonian matrix can be diagonalized as $\hat{H} = \alpha \hat{D} \alpha^{-1}$, with $D_{nm} = \delta_{nm} E_n$. The quasiparticles that diagonalize the Hamiltonian are the Bogoliubov quasiparticles,

$$\gamma_n = \sum_m \alpha_{nm}^{-1} c_m, \quad (3)$$

with energies E_n . By reexpressing the original creation-annihilation operators in terms of the Bogoliubov quasiparticles, one can recompute the parameters of the MF Hamiltonian. For example,

$$\begin{aligned} \langle n_{i\uparrow} \rangle &= \langle c_{i\uparrow}^\dagger c_{i\uparrow} \rangle = \sum_{nm} \langle \alpha_{i\uparrow,n}^* \gamma_n \alpha_{i\uparrow,m} \gamma_m \rangle \\ &= \sum_n |\alpha_{i\uparrow,n}|^2 n_F(E_n), \end{aligned} \quad (4)$$

where $n_F(E_n)$ is the Fermi-Dirac distribution function. Repeated until the convergence, the iterations produce the spatial profiles of the self-consistent density and order parameter.

A typical zero-temperature MF inhomogeneous solution is shown in Fig. 1. In the lowest energy configuration, the spin density develops a soliton-like AF anti-phase domain boundary — a stripe — at which the AF order parameter changes sign. At the domain boundary, the electronic charge density is depleted. The width of the domain wall, ξ_{DW} , decreases with increasing on-site repulsion U . However, for values of U that are not much larger than the hopping t , the charge per unit length of the optimal (the lowest energy) stripe remains the same and is close to unity near half-filling. This result, first demonstrated by Schultz [2], is a direct consequence of doping-dependent nesting in the Hubbard model. The bond-centered stripes are favored relative to the site-centered ones, although the energy difference in our case is small due to smooth charge distribution. For a different band structure the exact relation between the doping x and inter-stripe distance, $L(x)$, may change; however, any model whose ground state is AF at zero doping, is expected to have AF stripes for a finite doping, with incommensuration proportional to the doping, $1/L(x) \propto x$, near half-filling. For large enough doping levels, such that $L(x) \lesssim \xi_{DW}$, the AF stripes begin to overlap. In this regime the excitation spectrum is no longer fully gapped and mobile carriers appear. Further doping mostly changes the amplitude of the spin and charge density waves, only slowly modifying the incommensuration, $1/L(x)$ [2]. When the stripes are sufficiently close to melt, the AF aspect of the problem becomes unimportant, and the superconductivity is of the conventional BCS type.

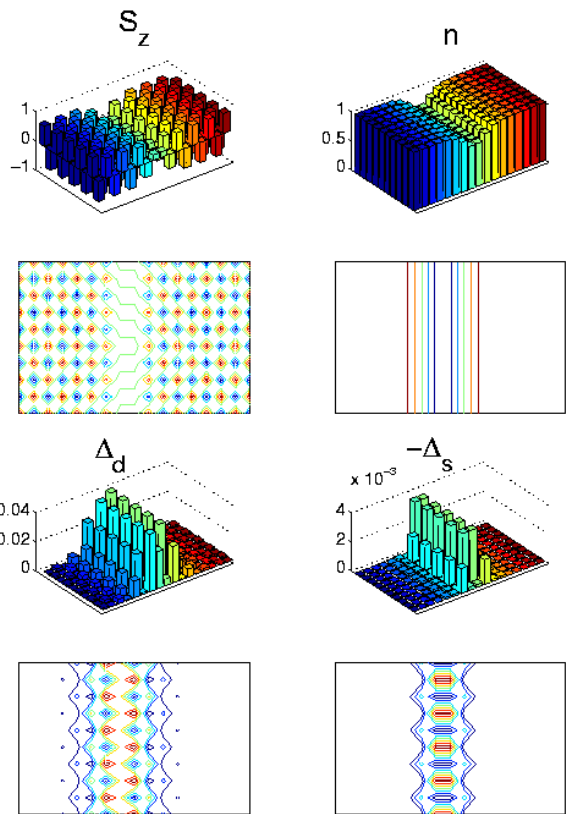


FIG. 1. Density and superconducting order parameter profiles in a stripe state (here period 17). The top two bar charts represent the site-dependent spin and charge densities, respectively. The contour plots indicate the sites with low (blue) and high (red) values of the corresponding densities. The bottom four plots show the values of the superconducting order parameters, defined as $\Delta_i^{d(s^*)} = (\Delta_{i,right} + \Delta_{i,left} \mp \Delta_{i,up} \mp \Delta_{i,down})/4$ for d -wave (extended s -wave) order parameter on site i ($U = 4t$, $V = -0.9t$). Different choices of parameters lead to qualitatively similar patterns, with stronger U leading to a stronger AF order and more attractive V causing the superconducting stripes to become wider and larger in amplitude. The doping level is 5.9%.

The superconducting order parameter $\Delta_{ij}^{d(s^*)}$ is maximal on the stripes and is not smooth (even within the stripe) due to the presence of the AF background. This happens since the order parameter is sensitive to the spin density on sites i and j . If i belongs to the spin-down sublattice and the neighbor j is on the spin-up sublattice, then the order parameter is large, and vice versa. Notice, that in addition to the dominant d -wave component, there is a small extended s -wave component generated on the stripe, which can be interpreted as a distortion of the d -wave at the level of about 10%. This happens because a symmetry of the lattice has been broken. The superconducting stripe is pinned by the AF phase domain boundary. Since the spin density on the domain boundary is small, a natural interpretation is that the

superconductivity is suppressed in the regions of large AF order. Nevertheless, the width of a superconducting stripe, ξ_{SC} , is determined not only by the width of the AF stripe, but also increases rapidly with increasing magnitude of the nearest neighbor attraction, V . For our choice of parameters, $\xi_{DW} \sim 4$ and $\xi_{SC} \sim 8$ lattice sites. For dopings smaller than about 10% (corresponding to $L(x) > 10$ lattice sites) the stripes have negligible overlap. In this regime, the amplitude of the superconducting order parameter on the stripes no longer depends upon the stripe-stripe separation. For higher doping levels, an overlap between the superconducting order parameters on the adjacent stripes is established.

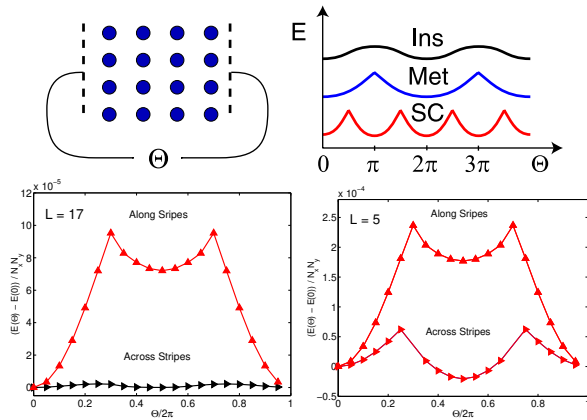


FIG. 2. (A) Schematics of typical energy spectra, $E(\Theta)$. The insulating behavior is characterized by a smooth curve of period 2π , with an amplitude that decays exponentially with system size. The metallic and the superconducting states typically have patterns with cusps, with variations in $E(\Theta)$ that decrease as a power of the system size in such a way that the charge stiffness, $D_c = \frac{L}{2} \partial^2 E / \partial \Theta^2$, remains constant. The superconducting behavior is distinguished from the metallic one by the reduced periodicity, referred to as anomalous flux quantization (AFQ). There is a direct correspondence between AFQ and the fact that the minimal flux that can penetrate a superconducting system is one half of the flux quantum, $\phi_0/2 = \hbar c/2e$. The exact period π is only achieved in the thermodynamic limit; for a finite system, there is only a signature of the reduced period. (B) Energy spectrum $E(\Theta)$ for a system of size 10×17 (see Fig. 1). *Along* the stripes there is a pronounced AFQ signature, which implies that the system is superconducting along the stripes. The energies were computed at a fixed chemical potential. To convert to the energy at a fixed average number of particles, a density adjustment by the amount $-\mu(n(\Theta)) - n(0)$ has been made. *Across* the stripes, the stiffness is extremely small, has a period of π , and does not have cusps. The scaling of D_c seems to imply that the system is an insulator, although a tiny superfluid density superconductor cannot be ruled out. (C) Energy spectrum $E(\Theta)$ for a system of size 10×15 with 3 stripes of period 5. Due to substantial overlap between the superconducting stripes, the system is superconducting both along and across the stripes.

A central question is connected to the conducting properties of the resulting inhomogeneous state: Is it a global superconductor, a metal, an insulator, or some unusual anisotropic phase? To resolve this issue we use the concepts of charge stiffness D_c [6], which measures the sensitivity of the ground state to changes in boundary conditions, and anomalous flux quantization [7], which provides a direct signature of the Meissner effect. These concepts, together with topological quantum numbers [8], are routinely employed to study the localization properties of models of interacting electrons. To compute D_c one needs to determine how the energy of a system with a fixed number of particles, E , depends on the twist in the boundary conditions, $\Theta \in [0, 2\pi]$. The twist of the boundary conditions is independently applied along each spatial direction $j = x, y$ and implies that $c_{N_j+1} = \exp(i\Theta)c_1$. The special case of $\Theta = 0$ corresponds to strictly periodic boundary conditions. Textbook schematics of the energy dependence, $E(\Theta)$, are shown in Fig. 2A. The many-particle spectrum $E(\Theta)$ for a system with a stripe separation of 17 lattice sites in our model is shown in Fig. 2B. The analysis of the energy curves implies that the system is superconducting in the direction along the stripes and insulating across the stripes. For a smaller stripe periodicity (Fig. 2C), due to substantial overlap between the stripes superconductivity is established in both directions, with an anisotropic superfluid density.

Arrays of superconductors separated by insulating regions, known as Josephson junction arrays, have non-trivial conducting properties. Depending on the strength of the coupling between the superconductors, such systems can be either superconductors or insulators [9]. In the case of superconducting channels separated by AF insulators, the coupling is inversely related to $L(x)$. For very large $L(x)$ at low doping, $L(x) \gg \xi_{SC}$, the overlap between the superconducting stripes, and hence the superconducting transition temperature T_c , is exponentially small. As the distance between the stripes decreases (larger doping), the overlap of the superconducting condensate wave functions should establish a phase coherent superconducting state. Indeed, this is qualitatively what we observe already at the mean-field level in the striped superconductors. For a large superconducting stripe overlap, the effective coupling between the stripes is non-exponential. In this regime, the superconducting transition temperature is proportional to incommensuration, which implies that the Josephson coupling should scale as $1/L(x)$ [10].

A possible experimental test of the Josephson-coupled superconductor scenario proposed here (see also [11]) can be performed by measuring the in-plane Josephson plasmon resonance. The resonance should be present in the microwave-frequency range and can be excited by an in-plane electric field.

From our zero-temperature analysis of the coexistence of AF stripes (ICAF) and superconductivity, a simple qualitative thermodynamic phase diagram emerges. In the conjectured phase diagram, we utilize the finite-temperature AF/ICAF phase diagram of the Hubbard model [2] and the superconducting phase diagram of the $t - V$ model [5]. For a suitable choice of parameters, for instance $U = 2t$ and $V = -t$, the superconducting (SC) and the AF/ICAF regions in the phase diagram intersect, as shown in Fig. 3. The boundary between the AF and ICAF phases corresponds to the $q = 0$ stripe modulation, and implies that the incommensuration is a decreasing function of temperature. The energy scale associated with the AF/ICAF region of the phase diagram is much larger than that of the SC part. Thus, one expects that only the SC phase boundary is modified when it passes through the AF/ICAF region. The central result of our work is that the superconductivity *does not* disappear in the region of the AF stripes, but rather becomes striped as well.

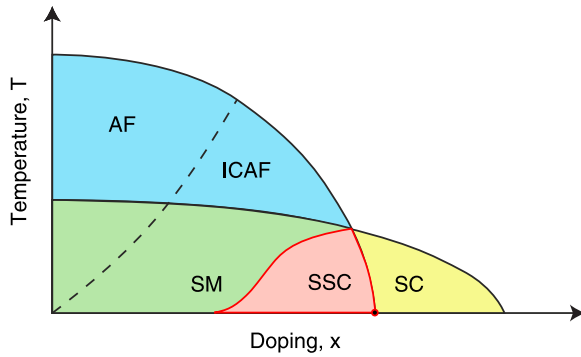


FIG. 3. Schematic phase diagram obtained by superimposing the antiferromagnetic/striped (AF/ICAF) and the d -wave superconducting (SC) phase diagrams. In the intersection region we distinguish the subregions of Josephson-coupled striped superconductor (SSC), and non-superconducting “strange metal” (SM), which is neither a superconductor, nor a simple insulator. The upper boundary of the AF/ICAF corresponds to the weak pseudogap crossover, and the line between the pure AF/ICAF and the SM demarcates the strong pseudogap crossover. In the very low doping region, the superconducting aspect of the problem becomes irrelevant, and the phase diagram is dominated by the physics of antiferromagnets.

Based on familiar Josephson coupling physics, in the region of coexistence of superconductivity and stripes, we can expect a part that is a globally coherent striped superconductor (SSC). The rest of the intersection region is covered by an exotic phase which, if it were perfectly orientationally ordered, would be a superconductor in one direction and a strongly-correlated insulator in the other. In reality, due to the meandering of the stripes and their break-up into finite segments [12], the state is likely to be

highly inhomogeneous and neither an insulator, nor a superconductor, but also not a simple metal. In agreement with the experimental attribution, we refer to this region as a “strange metal” (SM). The line separating the SM from the AF/ICAF region, in the context of the experiments, can be associated with the crossover to the strong pseudogap regime, and corresponds to the opening of the superconducting gap. The high-temperature AF/ICAF phase boundary demarcates the weak pseudogap. For very small dopings the MF stripe separation becomes so large that the superconducting aspects of the model become irrelevant and one crosses over to the regime governed predominantly by the physics of antiferromagnets.

It should be emphasized that the phase diagram presented here is based on the mean-field treatment of a 2-dimensional model. As such, it is susceptible to the quantum and thermal fluctuations that tend to destroy long-range order. For instance, the ICAF phase in Figure 3 in a real material is more likely to manifest itself as incommensurate AF fluctuations, rather than a pure phase. However, the effects of the 3rd dimension and impurity pinning may stabilize the mean-field phases at a sufficiently low temperatures, revalidating the mean-field phase diagram.

Within our model, we find that increasing on-site repulsion leads to a suppression of superconductivity. For larger U , the pure d -wave superconducting region of the phase diagram (SC) shrinks, and the width of the superconducting stripes in the SSC region decreases. This is in contrast with the homogeneous mean-field results [5], where the d -wave superconductivity is independent of the magnitude of U . On the other hand, large values of the on-site repulsion, $U > 4t$, in the Hubbard model lead to *diagonal* stripes [13]. Perhaps it is not a coincidence, that the insulating cuprates do in fact show diagonal stripes, as opposed to the lattice-aligned stripes in the superconducting cuprates.

There is an analogy between the role the doping plays in our model, and the strength of the electron-phonon coupling, λ , in the McMillan’s criterion for the maximum achievable T_c in conventional superconductors. In the McMillan’s picture, increasing λ favors superconductivity. However, increasing λ too much induces a structural transition, and hence changes the reference ground state. In our model, increasing doping brings the superconducting stripes closer together, and hence enhances the global T_c . However, increasing doping too much causes a transition to the uniform state, with a subsequent monotonically decreasing T_c as a function of doping.

The topology of the phase diagram proposed in this Letter appears to be relevant for the superconducting cuprates, such as LSCO and YBCO. The same simple model can produce other topologies as well. A non-trivial topology, which may be realized in a material with a weaker attractive coupling, is when the superconducting region is fully contained in the AF/ICAF region.

Depending on the parameters, such a material may be a striped superconductor in a certain range of dopings. Also, similar physics may occur in organic charge-transfer salts [14], that show AF, ICAF and superconductivity under pressure controlling interchain coupling.

In conclusion, we find that a simple one-band model with on-site repulsion and nearest-neighbor attraction, in an appropriate range of parameters, can simultaneously sustain both incommensurate antiferromagnetism and inhomogeneous superconductivity. Prompted by this finding and utilizing well-known antiferromagnetic and superconducting phase diagrams, we have constructed a generic phase diagram that captures many of the phases observed in the cuprate and organic superconductors. An experimental test of the Josephson-coupled superconductor proposed here (see also [11]) can be performed by measuring the in-plane Josephson plasmon resonance. Although our simple model appears to capture much of the observed rich physics, however it can be readily elaborated (multiple electron bands, 3-dimensionality, long-range interactions, lattice coupling, etc.) for more quantitative comparisons with specific materials.

We would like to thank L. Bulaevskii for suggesting to us the in-plane Josephson plasma experiment as a probe of the striped superconductivity. We acknowledge useful discussions with C.D. Batista, D. Morr, D. Pines, and S. Trugman. This work was supported by the U.S. DOE.

- [1] J. M. Tranquada *et al.*, Phys. Rev. B **52**, 3581 (1995); M. Arai *et al.*, Phys. Rev. Lett. **83**, 608 (1999); Z.-X. Shen *et al.*, Science **280**, 259 (1998).
- [2] H.J. Schulz, Phys. Rev. Lett. **64**, 1445 (1990).
- [3] J. Zaanen and O. Gunnarsson, Phys. Rev. B **40**, 7391 (1989).
- [4] D. Poilblanc and T. M. Rice, Phys. Rev. B **39**, 9749 (1989).
- [5] R. Micnas *et al.*, Rev. Mod. Phys. **62**, 113 (1990).
- [6] W. Kohn, Phys. Rev. **133**, A171 (1964).
- [7] N. Buyers and C. N. Yang, Phys. Rev. Lett. **7**, 46 (1961); A. Sudbo *et al.*, Phys. Rev. Lett. **70**, 978 (1993).
- [8] G. Ortiz and R. M. Martin, Phys. Rev. B **49**, 14202 (1994).
- [9] G. Schon and A.D. Zaikin, Phys. Rep. **198**, 237 (1990).
- [10] A. V. Balatsky and Z.-X. Shen, Science **284**, 1137 (1999).
- [11] J. Eroles *et al.*, Europhys. Lett. (2000); preprint cond-mat/0001430 (2000).
- [12] Kivelson, S.A. *et al.*, Nature **393**, 550 (1998); B. Stojkovic *et al.*, Phys. Rev. Lett. **82**, 4679 (1999).
- [13] H. J. Schulz, J. Phys. France **50**, 2833 (1989).
- [14] D. S. Chow *et al.*, Phys. Rev. Lett. **81**, 3984 (1998).